Chemistry & Biology *13*, 365–377, April 2006 ©2006 Elsevier Ltd All rights reserved DOI 10.1016/j.chembiol.2006.01.011

Biosynthesis of the Terpene Phenalinolactone in *Streptomyces* sp. Tü6071: Analysis of the Gene Cluster and Generation of Derivatives

Clemens Dürr,[1] Hans-Jörg Schnell,[1] Andriy Luzhetskyy,[1] Renato Murillo,[2] Monika Weber,[1] Katrin Welzel,[3] Andreas Vente,[3] and Andreas Bechthold[1,*]

[1] Albert-Ludwigs-Universität
Institut für Pharmazeutische Wissenschaften
Stefan-Meier-Strasse 19
79104 Freiburg
Germany

[2] Escuela de Quimica and CIPRONA
Universidad de Costa Rica
San José
Costa Rica

[3] Combinature Biopharm AG
Robert-Rössle-Strasse 10
13125 Berlin
Germany

Summary

Phenalinolactones are terpene glycosides with antibacterial activity. A striking structural feature is a highly oxidized γ-butyrolactone of elusive biosynthetic origin. To investigate the genetic basis of the phenalinolactones biosynthesis, we cloned and sequenced the corresponding gene cluster from the producer strain *Streptomyces* sp. Tü6071. Spanning a 42 kbp region, 35 candidate genes could be assigned to putatively encode biosynthetic, regulatory, and resistance-conferring functions. Targeted gene inactivations were carried out to specifically manipulate the phenalinolactones pathway. The inactivation of a sugar methyltransferase gene and a cytochrome P450 monooxygenase gene led to the production of modified phenalinolactone derivatives. The inactivation of a Fe(II)/α-ketoglutarate-dependent dioxygenase gene disrupted the biosynthetic pathway within γ-butyrolactone formation. The structure elucidation of the accumulating intermediate indicated that pyruvate is the biosynthetic precursor of the γ butyrolactone moiety.

Introduction

Streptomycetes continue to be the most prolific source for bioactive natural products [1]. In the past, research has been devoted in particular to polyketides and nonribosomal-derived peptides, of which many have found their way to market as indispensable antibiotic drugs. Yet an unprecedented increase in antimicrobial resistance makes the identification of structurally novel anti-infectives a demanding task, since new structures are promising to coincide with new mechanisms of action. The most chemically diverse pool of secondary metabolites in nature is constituted by terpenes [2]. However, the number of terpenoid natural products identified from *Streptomyces* is extremely limited. In 1956, novobiocin was isolated as the first antibiotic with a terpenoid side chain from *Streptomyces niveus* [3], followed by pentalenolactone from *Streptomyces* sp. with a pure terpenoid structure [4]. Until now only around 15 basic structures have been added to this limited pool, most of them being prenylated rather than pure terpenoid compounds [5]. Recently, the first biosynthetic gene cluster of an isoprene-derived natural product from a *Streptomyces* strain was reported with the terpentecin gene locus in *Streptomyces griseolosporeus* strain MF730-N6 [6, 7]. Interestingly, this cluster is located immediately upstream from the mevalonate pathway genes for isoprene biosynthesis. It was anticipated that this colocalization would efficiently supply the terpentecin pathway with isoprene building blocks. Most *Streptomyces* synthesize terpene natural products via the nonmevalonate pathway, the alternative route of isoprene biosynthesis [5]. However, until now there is no example of nonmevalonate pathway genes being associated with a secondary metabolite gene cluster.

Phenalinolactones A–D are terpene glycosides produced by *Streptomyces* sp. Tü6071 (Figure 1). The strain was first isolated by Gebhardt and Fiedler in 2001, and antibacterial activity of the phenalinolactones against a selection of gram-positive germs was demonstrated [8]. The structural elucidation was accomplished by Meyer and Zeeck in 2003, which revealed that the phenalinolactones constitute a unique composition of structural elements of novelty and biosynthetic interest [9]. The tricyclic *anti/anti/syn*-configured perhydrophenanthrene backbone consists of four isoprene units, of which the fourth comprises the β carbon of an intriguing γ-butyrolactone moiety (Figure 1). This structural element can be found in various sesterterpenoids from marine sponges, like the phospholipase A_2 inhibitors petrosaspongiolides from *Petrosaspongia nigra* [10]. The masked aldehyde function of the γ hydroxybutyrolactone was shown to covalently block phospholipase A_2 through the formation of a Schiff base with the N-terminal isoleucine residue [11]. The A ring of the phenalinolactones terpenoid scaffold is oxidatively functionalized, which allows the further decoration with an L-amicetose and a 5-methylpyrrole-2-carboxylic acid. The latter was shown to be the key pharmacophore of the potent gyrase inhibitor clorobiocin from *Streptomyces roseochromogenes* [12]. Particularly striking is the oxygen function at C-3, which is further acetylated. Its presence hints at an epoxidation of the linear terpene chain prior to its cyclization, analogous to eukaryotic sterol formation. Although a handful of prokaryotes have been reported to be capable of sterol production [13], this would be without precedent for natural product biosynthesis in bacteria.

Herein, we report the cloning, sequencing, and functional analysis of the phenalinolactones biosynthetic gene cluster in *Streptomyces* sp. Tü6071. In an effort to examine details of the phenalinolactones biosynthesis, knockout mutants were generated for a methyltransferase gene (*plaM1*), two oxygenase genes (*plaO1* and *plaO4*), and three genes involved in the formation of

*Correspondence: andreas.bechthold@pharmazie.uni-freiburg.de

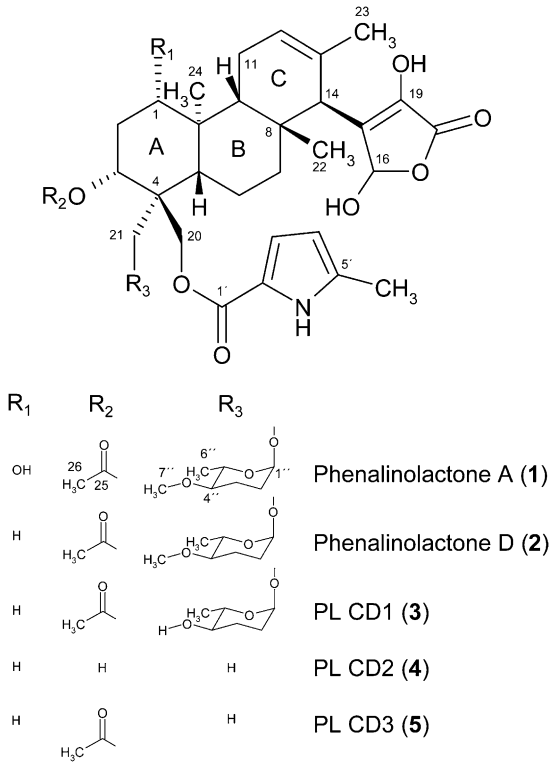

Figure 1. Chemical Structures of Phenalinolactones

Phenalinolactone A (1) and D (2) are the principal metabolites of *Streptomyces* sp. Tü6071. The new derivatives PL CD1 (3), PL CD2 (4), and PL CD3 (5) were produced by engineered mutant strains.

the phenalinolactones backbone (*plaT1*, *plaT2*, and *plaT3*). The structure elucidation of derivatives that accumulated in the mutant strains, together with the annotation analysis of the cluster sequence, leads to a detailed proposal for major parts of phenalinolactone biosynthesis.

Results and Discussion

Cloning and Identification of the Gene Cluster

The formation of the deoxyhexose L-amicetose during phenalinolactone biosynthesis requires the presence of an NDP-glucose-4,6-dehydratase gene [14]. Therefore 2304 *Escherichia coli* DH5α colonies containing a cosmid library of the producers genome were screened with a strain-specific NDP-glucose-4,6-dehydratase gene probe. Cosmid DNA from 21 positively hybridizing clones was subsequently analyzed by restriction mapping. This revealed that a group of six cosmids contained overlapping DNA. Fragments derived from this group were subcloned and sequenced. Guided by restriction and sequence analysis, two overlapping cosmids, 3-1O12 and 10-4D08, were selected for complete shotgun sequencing. From the obtained sequence data, a contiguous region of 49.4 kbp could be assembled. The *pla* gene cluster was assigned to 42 kbp within this region, with flanking regions of 6.5 kbp upstream and 1 kbp downstream of the clusters assumed boundaries. The overall G/C content is 70.5 mol %, matching the typical range of DNA from *Streptomyces*. Within coding sections, the G/C frequency is significantly increased at the codons' third position, simplifying the identification of potential ORFs by using the G/C frame plot method [15]. The annotation analysis revealed 35 candidate genes putatively encoding biosynthetic, regulatory, and resistance-conferring functions (Figure 2). The closest homologs of the annotated genes and their proposed functions are compiled in Table 1.

Genes/Enzymes Putatively Involved in Terpene Biosynthesis

The genes *plaT5* and *plaT6* encode proteins that are highly similar to the nonmevalonate pathway enzymes1-hydroxy-2-methyl-2-(E)-butenyl-4-diphosphate (HMBPP) synthase and 1-deoxy-D-xylulose-5-phosphate (DXP) synthase, respectively. DXP synthase catalyzes the initial step of this pathway: the formation of DXP by condensation of pyruvate and glyceraldehyde 3-phosphate. HMBPP synthase controls the second-to-last step in converting 2-*C*-methyl-D-erythritol-2, 4-cyclodiphosphate into HMBPP [16]. To the best of our knowledge, this is the first example of nonmevalonate pathway genes being embedded in a secondary metabolite gene cluster.

The product of *plaT4* is most similar to the terpene synthase ORF1 from the terpentecin producer *S. griseolosporeus* strain MF730-N6. Incubation of purified ORF1 with isopentenyl diphosphate and dimethylallyl diphosphate was shown to yield geranylgeranyl diphosphate (GGDP) [6]. A particularly interesting gene is *plaT1*, which encodes a putative monoxygenase with a conserved FAD binding motif. PlaT1 shows end-to-end similarities greater than 40% to a multitude of eukaryotic squalene epoxidases. A recent bioinformatoric approach identified only two prokaryotic organisms to be equipped with squalene epoxidase genes [17]. The product of *plaT2* resembles several putative squalene cyclases. Interestingly, PlaT2 lacks the highly acidic protonation motif, DxDD, which is proposed to enable the direct protonation of the terminal double bond of squalene that initiates the cationic cyclization reaction [18]. This motif is also absent in eukaryotic oxidosqualene cyclases, where prior epoxidation of the substrate facilitates the protonation-initiated cyclization. Hence, the lack of this motif in PlaT2 supports a sterol-like cyclization reaction within phenalinolactone biosynthesis, as already indicated through the presence of the putative epoxidase gene *plaT1*. The gene *plaT3* encodes a protein homologous to polyprenyltransferases found in association with ubiquinone biosynthesis. PlaT3 might be considered to transfer the phenalinolactones terpene scaffold on the biosynthetic precursor of the γ-butyrolactone moiety.

Genes/Enzymes Putatively Involved in Biosynthesis and Transfer of L-Amicetose

Recently, the rational combination of deoxysugar biosynthetic genes from different organisms was successfully applied to direct amicetose biosynthesis [19]. In the phenalinolactone cluster, we describe for the first time the complete gene set for the formation of this rare deoxyhexose. Eight genes can reliably be predicted to encode biosynthesis and transfer of this sugar moiety. The reaction scheme, as can be deduced from the sequence

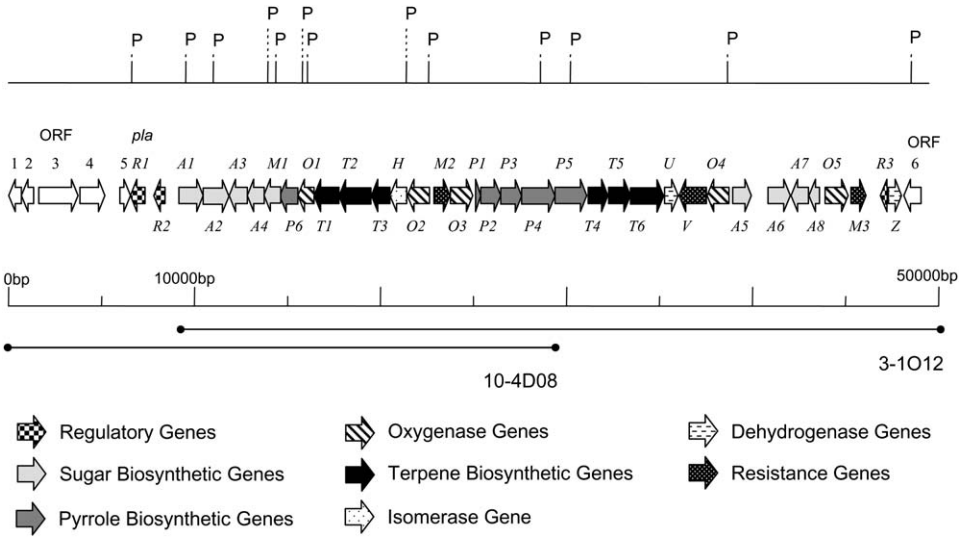

Figure 2. Genetic Organization of the Phenalinolactone Gene Cluster in *Streptomyces* sp. Tü6071

The contiguous sequence derives from two overlapping cosmids, 3-1O12 and 10-4DO8, the boundaries of which are outlined. P = PstI restriction sites.

analysis, is congruent with the pathway of L-rhodinose, the second naturally occurring tridesoxyhexose [20]. L-rhodinose differs from L-amicetose only in the stereoconfiguration at C-4. The multistep conversion of glucose-1-phosphate to NDP-L-amicetose includes NDP-D-glucose synthesis (PlaA4), a 4,6-dehydratation (PlaA3), a 2,3-dehydratation (PlaA2), a 3-ketoreduction (PlaA5), and a 3-deoxygenation step (PlaA1), to yield NDP-D-cinerulose. The final steps are 5-epimerization (PlaA8) and stereospecific 4-ketoreduction (PlaA7) toward NDP-L-amicetose. Finally, the attachment of NDP-L-amicetose to O-21 is likely catalyzed by PlaA6, which resembles many natural product glycosyltransferases. The candidate enzyme for the further modification of the sugar ligand through 4-*O*-methylation is PlaM1, with a high degree of sequence identity to NanM, a putative rhodinosyl-4-*O*-methyltransferase from *Streptomyces nanchangensis* [21].

Genes/Enzymes Putatively Involved in Biosynthesis and Transfer of 5-Methylpyrrole-2-Carboxylic Acid

A group of four genes was identified (*plaP2–plaP5*) that can be assigned to encode biosynthesis and transfer of the 5-methylpyrrole-2-carboxylic acid. The formation of this pyrrole ligand has been studied in detail in the context of clorobiocin biosynthesis in *S. roseochromogenes* [22–24]. The average end-to-end similarity with the homolog genes from the clorobiocin cluster (*cloN2–cloN6*) is almost 80%. Thus, an analog pathway can be anticipated. However, a major difference is constituted by PlaP4, in which the functions of the free-standing L-prolyl-AMP-ligase CloN4 and the small peptidyl carrier protein (PCP), CloN5, are combined. CloN4 was shown to convert L-proline into its acyl adenylate and then transfer the prolyl moiety on the phosphopantetheinyl arm of CloN5. Thus, PlaP4 exhibits the architecture of a nonribosomal peptide synthetase, with a C-terminal adenylation (A−) domain and a PCP domain located at the N terminus. PlaP3, homologous to the flavoprotein dehydrogenase CloN3, would catalyze the four electron oxidation of the PlaP4 bound proline toward the aromatic pyrrolyl-2-carboxy-*S*-PlaP4 product. PlaP2 is the homolog of the acyltransferase CloN2, which was recently shown to be involved in the transfer of the pyrrole-2-carboxylic acid to 3-OH of the deoxysugar in clorobiocin biosynthesis [24]. Accordingly, PlaP2 would catalyze the transfer of the pyrrole ligand to O-20 of the phenalinolactones terpene scaffold. PlaP5 shares conserved sequence motifs with the radical SAM protein superfamily, and is the homolog of CloN6, which was shown to methylate C-5 of the pyrrole ligand [23]. It is interesting to note that the *cloN2* mutant of *S. roseochromogenes* accumulated only pyrrole-2-carboxylic acid, but not its 5-methyl derivative [24]. This indicates that C-5 methylation of the pyrrole ligand does not occur prior to its transfer to the clorobiocin molecule.

Oxygenase Genes/Enzymes

One Fe(II)/α-ketoglutarate-dependent dioxygenase gene (*plaO1*) and four cytochrome P450 monoxygenase (*plaO2–O5*) genes can be found within the *pla* gene cluster. PlaO2–PlaO5 each possess the conserved heme binding sequence FGxGxHxCLG, with the invariant cysteine residue and regions homologous to the O_2 binding motif LLxAGxxS/T [25]. The homologs of the monoxygenases PlaO2, PlaO3, and PlaO5 were shown to hydroxylate aliphatic carbon atoms, whereas the homolog of PlaO4 was shown to oxidize a conjugated double bond, which is part of a polyunsaturated macrolactone (for references, see Table 1). Thus, we initially assigned PlaO2, PlaO3, and PlaO5 to the hydroxylations of the phenalinolactones aliphatic A-ring and PlaO4 to the hydroxylation at C-19 of the γ-butyrolactone.

The dioxygenase PlaO1 exhibits the characteristic HxD-signature for the coordination of α-ketoglutarate. Fe(II)/α-ketoglutarate-dependent dioxygenases participate in a multitude of biosynthetic reactions coupling the decarboxylation of α-ketoglutarate to the oxidation

Table 1. Deduced Functions for Genes in the Phenalinolactone Gene Cluster

Protein	Amino Acids	Homolog	ID%/SI%	Accession No.	Proposed Function	Reference
ORF1	228	TrkB (*Mycobacterium avium*)	58/77	NP_961743.1	K^+-transporter	
ORF2	222	TrkA (*Propionibacterium acnes KPA171202*)	55/72	YP_055767	K^+-transporter	
ORF3	702	Putative amino acid permease (*Streptomyces avermitilis* MA-4680)	83/91	BAC70101	Amino acid transporter	
ORF4	447	Putative RNA methyltransferase (*Streptomyces coelicolor* A3[2])	80/88	CAA16438	tRNA-5-uracil-methyltransferase	
ORF5	190	Putative transposase (*Streptomyces coelicolor* A3[2])	71/80	CAB45597	Transposase	
PlaRI	265	MonRI (*Streptomyces cinnamonensis*)[a]	83/89	AAO65809	Regulator	[29]
PlaR2	200	Putative TetR-family transcriptional regulator (*Streptomyces coelicolor* A3[2])	40/53	CAC44278	Regulator	
PlaA1	434	UrdQ (*Streptomyces fradiae*)[a]	80/87	AAF72550	3-Deoxygenation	[20]
PlaA2	463	LanS (*Streptomyces cyanogenus*)	61/72	AAD13549	2,3-Dehydratase	[44]
PlaA3	323	MtmE (*Streptomyces argillaceus*)	69/78	T48867	4,6-Dehydratase	[45]
PlaA4	301	NanG1 (*Streptomyces nanchangensis*)	74/85	AAP42866	Nucleotidylyl-transferase	[21]
PlaM1	303	NanM (*Streptomyces nanchangensis*)	61/77	AAP42862	Methyltransferase	[21]
PlaP6	321	CloN7 (*Streptomyces roseochromogenes* ssp. oscitans)	53/69	AAN65236	Hydrolase	[46]
PlaO1	288	TauD (*Pseudomonas putida*)[a]	42/59	BAC00965.1	Dioxygenase	[47]
PlaT1	449	Squalene epoxidase (*Rattus norvegicus*)[a]	23/41	NP_058832.1	Epoxidase	[48]
PlaT2	571	Putative squalene cyclase (*Rubrobacter xylanophilus* DSM 9941)	31/45	ZP_00200293	Cyclase	
PlaT3	337	Putative prenyltransferase (*Rubrobacter xylanophilus* DSM 9941)	38/51	ZP_00200292	Prenyltransferase	
PlaH	294	BorN (*Streptomyces parvulus*)[a]	44/56	CAE45678	2-Hydroxyhept-2,4-diene-1,7-dioate isomerase	[32]
PlaO2	397	EncR (*Streptomyces maritimus*)[a]	40/54	AAF81737	Cytochrome P450 monoxygenase	[49]
PlaM2	281	Putative rRNA-methyltransferase (*Streptomyces coelicolor* A3[2])	54/67	NP_628799	Self-resistance	
PlaO3	401	EryK (*Aeromicrobium erythreum*)[a]	47/63	AAU93795	Cytochrome P450 monoxygenase	[50]
PlaP1	96	CloN1 (*Streptomyces roseochromogenes* ssp. oscitans)	57/65	AAN65230	Hypothetical protein	[46]
PlaP2	355	CloN2 (*Streptomyces roseochromogenes* ssp. oscitans)[a]	68/81	AAN65231	Acyltransferase	[24]
PlaP3	377	CloN3 (*Streptomyces roseochromogenes* ssp. oscitans)[a]	70/81	AAN65232	Dehydrogenase	[22]
PlaP4	594	CloN4 aa 1–498[a]	68/78	AAN65233	Acyl-CoA synthetase	[22]
		CloN5 aa 507–594 (*Streptomyces roseochromogenes* ssp. oscitans)[a]	61/76	AAN65234	Peptidyl-carrier protein	[22]
PlaP5	568	CloN6 (*Streptomyces roseochromogenes* ssp. oscitans)[a]	81/90	AAN65235	Methyltransferase	[46]
PlaT4	359	GGDPS (*Kitasatospora griseola*)[a]	46/59	BAB07816	GGDP synthase	[6]
PlaT5	386	GcpE (*Mycobacterium avium*)	73/84	NP_961872	HMBPP synthase	
PlaT6	593	DXS (*Kitasatospora griseola*)	55/66	BAB20589	DXP synthase	
PlaU	244	ChnA (*Brevibacterium epidermidis* sp. HCU)[a]	41/53	AAK73164	Dehydrogenase	[33]
PlaV	484	EstB (*Burkholderia gladioli*)[a]	29/42	AAF59826	Self-resistance	[31]
PlaO4	391	PimD (*Streptomyces natalensis*)[a]	41/55	CAC20932	Cytochrome P450 monoxygenase	[25]
PlaA5	335	Gra-orf26 (*Streptomyces violaceoruber*)[a]	55/66	CAA09647	3-Ketoreductase	[51]
PlaA6	396	MtmGIII (*Streptomyces argillaceus*)	35/51	AAD55583	Glycosyl-transferase	[52]
PlaA7	311	TylCIV (*Streptomyces fradiae*)	50/63	AAD41822	4-Ketoreductase	[53]
PlaA8	191	LndZ1 (*Streptomyces globisporus*)	53/69	AAT37542	3,5-Epimerase	
PlaO5	409	PicK (*Streptomyces venezuela*)[a]	43/56	AAC64105	Cytochrome P450 monoxygenase	[54]
PlaM3	270	Putative rRNA-methyltransferases (*Streptomyces coelicolor* A3[2])	50/63	NP_628799	Self-resistance	
PlaR3	119	Putative transcriptional regulator (*Nocardia farcinica* IFM 10152)	55/71	YP_117420	Regulator	
PlaZ	237	Putative short-chain dehydrogenase (*Rhizobium leguminosarum*)	38/54	AAL14912	Dehydrogenase	
ORF6	311[b]	AnsG oxidoreductase (*Streptomyces collinus*)	40/51	AAD31836	Oxidoreductase	[55]

[a] Function experimentally established.
[b] *orf* incomplete.

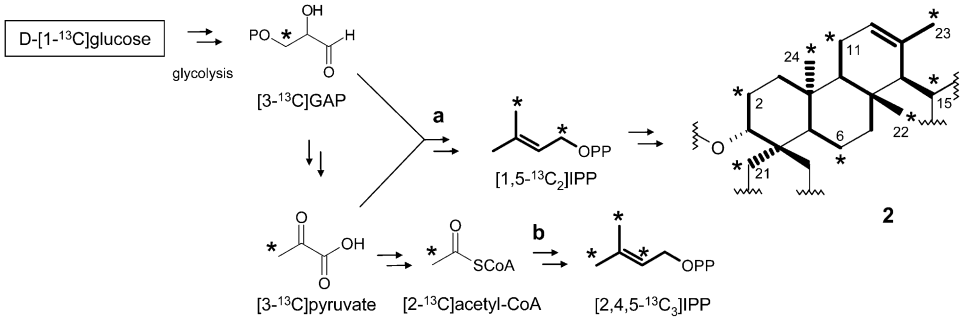

Figure 3. Labeling of the Diterpene Scaffold of **2** from D-[1-^{13}C]glucose Feeding

Phenalinolactone D (**2**) was isolated from liquid cultures of *Streptomyces sp.* Tü6071 supplied with D-[1-^{13}C]glucose. The labeling pattern observed in the terpene scaffold of **2** documents that the IPP units are synthesized via the nomevalonate pathway (**a**) and not via the acetate-mevalonate pathway (**b**). Asterisk indicates ^{13}C atoms.

of carbon atoms [26]. A prominent example for the versatility of this class of enzymes is the clavaminate synthase, which catalyzes three separate oxidative steps in the biosynthesis of clavulanic acid [27]. The reactions comprise hydroxylation, dehydration, and oxidative cyclization. All these types of reaction can be assumed to occur during the formation of the phenalinolactones γ-butyrolactone moiety.

Genes/Enzymes Putatively Involved in Regulation and Self-Resistance

Located at the 5′-end of the cluster is *plaR1*, which encodes a protein with high end-to-end similarity to regulatory proteins from the SARP family [28]. SARPs interact with characteristic heptameric tandem repeat sequences upstream of biosynthetic genes to activate transcription. The OmpR-like helix-turn-helix consensus motif for DNA binding, strongly conserved in members of the SARP family, is present in PlaR1. A potential DNA binding site (TCGAGCG-N_{12}-TCGAGCG) could be found upstream of *plaA5*. The closest homolog is the activator MonRI from *Streptomyces cinnamonensis*, which was shown to significantly increase monensin production after overexpression [29]. Downstream follows *plaR2*, which encodes another putative transcriptional regulator homologous to the TetR family. To the same family belongs the gene product of *plaR3*, the third putative regulatory gene, which is located almost at the 3′ end of the cluster.

Three genes (*plaM2*, *plaM3*, and *plaV*) can be considered to confer phenalinolactone resistance to the producing organism. PlaM1 and PlaM2 resemble rRNA-methyltransferases, which are common resistance determinants in antibiotic producers. They prevent the binding of the antibiotic to the ribosome by methylating its specific target site [30]. This would indicate that the phenalinolactones interfere with protein biosynthesis. An additional resistance mechanism might be established by *plaV*, which encodes a putative hydrolase. Among a multitude of β-lactamases, PlaV is similar to the hydrolase EstB from *Burkholderia gladioli,* which adopts a β-lactamase fold but has esterolytic activity. It was shown that EstB deacetylates 7-aminocephalosporinic acid [31]. Three ester functions in the phenalinolactones structure can be considered as target for PlaV. In particular, ester hydrolysis of the γ-butyrolactone or cleavage of the pyrrole carboxylic ester, both known to be crucial pharmacophores in other compounds, would likely be accompanied by the loss of the phenalinolactones biological activity.

Other Genes/Enzymes

The product of *plaH* shows homology to 2-hydroxyhepta-2,4-diene-1,7-dioate isomerase (HHDI), a key enzyme of the tyrosine catabolism *via* the 4-hydroxyphenylacetic acid pathway. HHDI catalyzes the tautomerization of 2-hydroxyhepta-2,4-diene-1,7-dioate to 2-oxohepta-3-ene-1,7-dioate. For the closest homolog, BorN from the borrelidin producer, *Streptomyces parvulus* Tü4055, it was suggested that the enzyme diverges 2-oxohepta-3-ene-1,7-dioate from primary metabolism to borrelidin biosynthesis. This channeling function was corroborated through inactivation of *borN*, which led to a decreased, but not abolished, borrelidin production [32]. The products of *plaU* and *plaZ* both contain domains of short-chain dehydrogenases (Pfam00106) and enoyl-[acyl carrier protein] reductases (COG0623). The closest homolog of PlaU is the dehydrogenase, ChnA, which is involved in the oxidative degradation of cyclohexanol. ChnA catalyzes the dehydrogenation of cyclohexanol toward cyclohexanone [33]. Finally, *plaP1* and *plaP6* encode the homologs of the hypothetical protein, CloN1, and the putative hydrolase, CloN7, from *S. roseochromogenes*, respectively. *cloN1* and *cloN7* are located within the operon for pyrrole-2-carboxylic acid biosynthesis, but their functions have not yet been established.

Isotope Feeding

The presence of the *plaT5* and *plaT6* genes implies that the phenalinolactones isoprene building blocks are synthesized via the nonmevalonate pathway. To confirm this, we fed D-[1-^{13}C]glucose to cultures of *Streptomyces* sp. Tü6071. The catabolism of D-[1-^{13}C]glucose via glycolysis yields [3-^{13}C]glyceraldehyde-3-phosphate (GAP) and [3-^{13}C]pyruvate, the starting material for the nonmevalonate pathway (Figure 3). The latter yields [2-^{13}C]acetate after decarboxylation. [3-^{13}C]GAP and [3-^{13}C]pyruvate enter the nonmevalonate pathway, giving rise to isoprene (IPP) monomers labeled at carbons 1 and 5 [34]. The alternative acetate-mevalonate route would utilize [2-^{13}C]acetate, leading to [2,4,5-^{13}C_3]IPP

units. Compared to the natural abundance, the ^{13}C-NMR analysis of compound **2** (Figure 1) isolated from the D-[1-^{13}C]glucose feeding showed that, within the terpene scaffold, carbons 2 (5.0), 6 (4.9), 11 (5.2), 15 (3.4), 21 (3.8), 22 (4.9), 23 (5.1), and 24 (4.9) were enriched (relative enrichments in parentheses). This matches the expected labeling pattern that arises from [1,5-$^{13}C_2$]IPP units. Hence, we can document that the phenalinolactones terpene scaffold comprises four isoprene monomers supplied via the nonmevalonate pathway.

Generation of Mutant Strains

In order to document the involvement of the *pla* gene cluster in phenalinolactone biosynthesis, we sought the rational design of a novel phenalinolactone derivative by targeted gene inactivation. A promising candidate for this approach was the putative sugar methyltransferase gene, *plaM1*. Inactivation of this class of genes has successfully been applied to generate novel derivatives in other systems [35, 36]. Further gene inactivations were carried out to gain insight into the formation of the phenalinolactones core structure, including the striking γ-butyrolactone moiety. Therefore, we selected genes that we assumed to be involved in the assembly of the terpene backbone (*plaT1*, *plaT2*) and in the biosynthesis of the γ-butyrolactone (*plaT3*, *plaO1*, *plaO4*). The mutations were achieved either by deletion of an internal fragment (*plaM1*, *plaO1*, *plaO4*, *plaT1*) or by a shift of the reading frame (*plaT1*, *plaT2*). Inactivation plasmids were introduced into the wild-type' s chromosome by means of homologous recombination. The single- and double-crossover recombination events were documented by PCR analysis. All mutant strains were subsequently complemented in *trans* with a full-length copy of the respective gene under control of the constitutive promoter, *ermE**. This restored wild-type production to full levels in all mutant strains (for detailed protocols for the generation of inactivation and complementation plasmids, and for PCR analysis, see the Supplemental Data available online).

Inactivation of *plaM1*

The production profile of the mutant strain *Streptomyces* sp. Tü6071 ΔplaM1 was analyzed by HPLC/electrospray ionization (ESI)-MS at a detection wavelength of λ = 280 nm and compared to that of the wild-type. The wild-type produced phenalinolactones A and D as major metabolites with retention times (RT) of 21.4 and 24.5 min and molecular ions of *m/z* 714 $[M-H]^-$ and *m/z* 698 $[M-H]^-$, respectively (**1** and **2**, Figure 4). Both were absent in the mutant, which instead produced a novel main compound at RT = 21.8 min, with the typical UV/VIS spectrum of the phenalinolactones chromophore, referred to as PL CD1 (**3**, Figure 4). The corresponding molecular ion of *m/z* 684 $[M-H]^-$ reflected a mass difference of 14 amu in reference to **2**, consistent with the envisaged loss of a methyl group. To locate the position of the missing methyl group, **3** was purified from an upscaled fermentation and subjected to ^{1}H-NMR spectroscopy. As expected, the distinct methoxy singlet of the 4″-*O*-CH_3 group at δ 3.51 was absent in the ^{1}H-spectrum of **3**. Thus, **3** lacking the sugar methyl group was clearly identified as the progenitor of **2**. This result documents that PlaM1 is an L-amicetosyl-4″-*O*-methyltransferase and thereby unambiguously proves that the cloned gene cluster encodes phenalinolactone biosynthesis. Interestingly, an unmethylated variant of **1**, the wild-types main derivative, was observed in the mutant only in traces (data not shown). This implies that hydroxylation at C-1 occurs after methylation of the sugar ligand, since the involved oxygenase seems to be inefficient in utilizing **3** as substrate.

Inactivation of *plaT1*, *plaT2*, and *plaT3*

The analysis of the mutants' extracts by HPLC/ESI-MS revealed that, in all cases, phenalinolactone production was abolished completely, without leading to the accumulation of any detectable intermediates. This underlines that PlaT1, PlaT2, and PlaT3 are essential for phenalinolactone formation, but their respective functions remain to be resolved.

Inactivation of *plaO4* and *plaO1*

The HPLC/ESI-MS analysis of the mutant strain *Streptomyces* sp. Tü6071 ΔplaO4 revealed two novel main compounds at RT = 18.3 and 21.4 min labeled as PL CD2 and PL CD3, respectively (**4** and **5**, Figure 4). In both compounds the characteristic UV/VIS-spectrum of the phenalinolactones was precisely conserved. The corresponding molecular masses were determined with *m/z* 512 $[M-H]^-$ for **4** and *m/z* 554 $[M-H]^-$ for **5**. To elucidate the underlying structure, **4** was purified from an upscaled fermentation and subjected to 1D (^{1}H, ^{13}C) and 2D (^{1}H-^{1}H-COSY, HSQC, HMBC) NMR spectroscopy. The analysis of the ^{1}H and ^{13}C spectra revealed the absence of the signals for the sugar and the acetyl moiety. Instead, a novel signal corresponding to a methyl group showed up in the ^{1}H spectrum at δ 0.79. ^3J correlations to C-3, C-5, and C-20, and a ^2J correlation to C-4, observed in the HMBC spectrum clearly identified this novel methyl group to be linked to the quaternary carbon at C-4. The chemical shift of the corresponding carbon signal at δ 12.9 documents the axial position of this methyl group [37]. This explains the lack of the sugar signals, since this methyl group needs to undergo oxidation first, before the *O*-glycosidic sugar transfer can take place. Other than expected, the structure of **4** (Figure 1) identified PlaO4 to be the oxygenase that hydroxylates C-21 during phenalinolactone biosynthesis. The mass difference of 42 amu suggests that **5** (Figure 1) is the 3-O-acetylated congener of **4**.

Upon HPLC/ESI-MS analysis of the mutant *Streptomyces* sp. Tü6071 ΔplaO1 at a detection wavelength of λ = 235 nm two novel compounds, now referred to as PL CD6 and PL CD7 (**6** and **7**, Figure 4), could be detected at RT = 18.1 min and RT = 20.2 min with molecular ions of *m/z* 373 $[M-H]^-$ and *m/z* 371 $[M-H]^-$, respectively (Figure 4, A). Both compounds displayed the same UV/VIS spectrum which differed fundamentally from that of the phenalinolactones chromophore (Figure 4, B). An intense tailing of the corresponding peaks in the reversed-phase chromatography suggested the presence of an acidic function. For structure elucidation, both derivatives were purified from an upscaled fermentation and subsequently submitted to high-resolution ESI-MS. The observed molecular ions were *m/z* 373.2384 $[M-H]^-$ for **6** and *m/z* 371.2233 $[M-H]^-$ for **7**, indicating sum

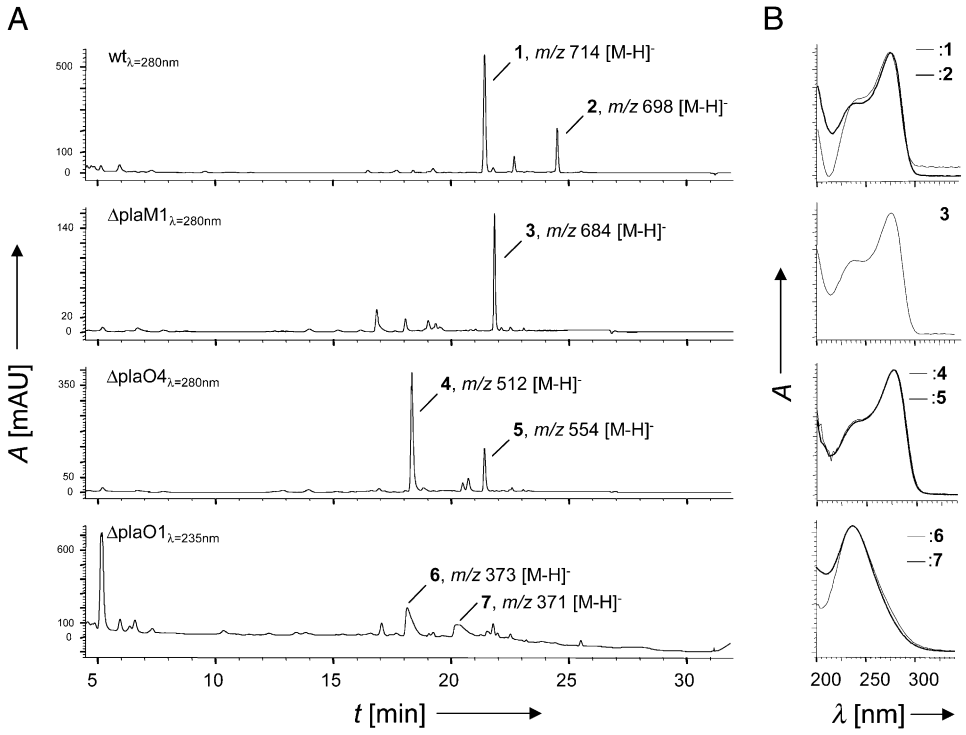

Figure 4. Production Analyses of *Streptomyces* sp. Tü6071 and Its Mutant Strains

(A) HPLC traces of crude extracts of *Streptomyces* sp. Tü6071 (wt) and its mutant strains *Streptomyces* sp. Tü6071 ΔplaM1 (ΔplaM1), *Streptomyces* sp. Tü6071 ΔplaO4 (ΔplaO4), and *Streptomyces* sp. Tü6071 ΔplaO1 (ΔplaO1).

(B) UV/VIS spectra of the respective main metabolites.

formulae of $C_{23}H_{33}O_4$ $[M\text{-}H]^-$ (calculated: *m/z* 373.2379) and $C_{23}H_{31}O_4$ $[M\text{-}H]^-$ (calculated: *m/z* 371.2222), respectively. The mass difference of Δm = 2.0157 amu, matching the mass of two protons, suggested that **6** and **7** constitute a redox pair of a common basic structure.

The subsequent NMR analyses identified **6** as the almost unmodified diterpenoid core of the phenalinolactones extended with a C_4 side chain attached to C-14 (Figure 5). The signals of the methyl groups at C-19, C-20, C-21, C-22, and C-23 could be assigned based on their respective ^3J correlations to the core carbon atoms observed in the HMBC spectrum. The characteristic signals of the γ-butyrolactone portion were absent. Instead, proton signals of a novel double bond appeared. The *trans* configuration of this double bond was reflected in the coupling constant value of $^3J_{H15–H16}$ = 16 Hz. The placement of this olefin in **6** was ascertained through correlation from H-15 to H-14 observed in the $^1H^1H$-COSY, with $^3J_{H15–H14}$ = 11 Hz. The observation of the ^{13}C-NMR spectrum at low temperature (248K) allowed the detection of two carbon signals at δ 168.5 (C18) and δ 191.0 (C17), correlating to a carboxylic acid and a ketone, respectively. Long-range correlations $^3J_{H14–C16}$, $^3J_{H15–C17}$, $^2J_{H16–C17}$, and $^3J_{H16–C18}$ established the partial structure of a β,γ-unsaturated α-keto acid linked to C-14. The presence of the OH function at C-3 was reflected in the chemical shift of δ 3.13 for H-3, consistent with its attachment to a carbon bearing a heteroatom. The axial position of H-3 could be determined due to the coupling constant values of 11 Hz and 5 Hz, indicating an axial-axial and an axial-equatorial coupling to H_{ax}-2 and H_{eq}-2, respectively. Thus, 3-OH is in equatorial position as it is the 3-O-acetyl substituent in **1**. A further

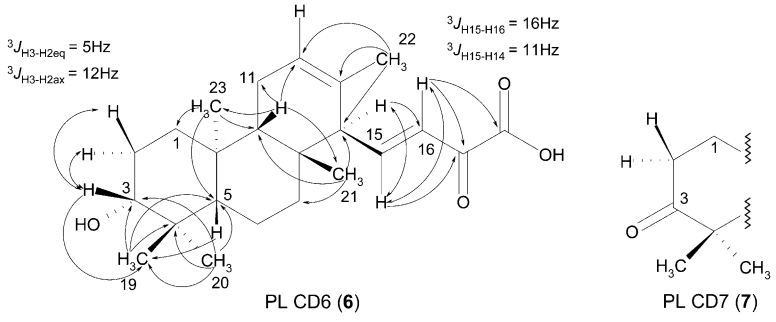

Figure 5. Structure Elucidation of PL CD6 and PL CD7

Single-headed arrows indicate $^3J_{HC}$ long-range couplings observed by HMBC experiments, double-headed arrows represent $^3J_{HH}$ couplings observed in the $^1H/^1H$-COSY spectrum. Crucial $^3J_{HH}$ coupling constants are specified. **6**, PL CD6; **7**, PL CD7.

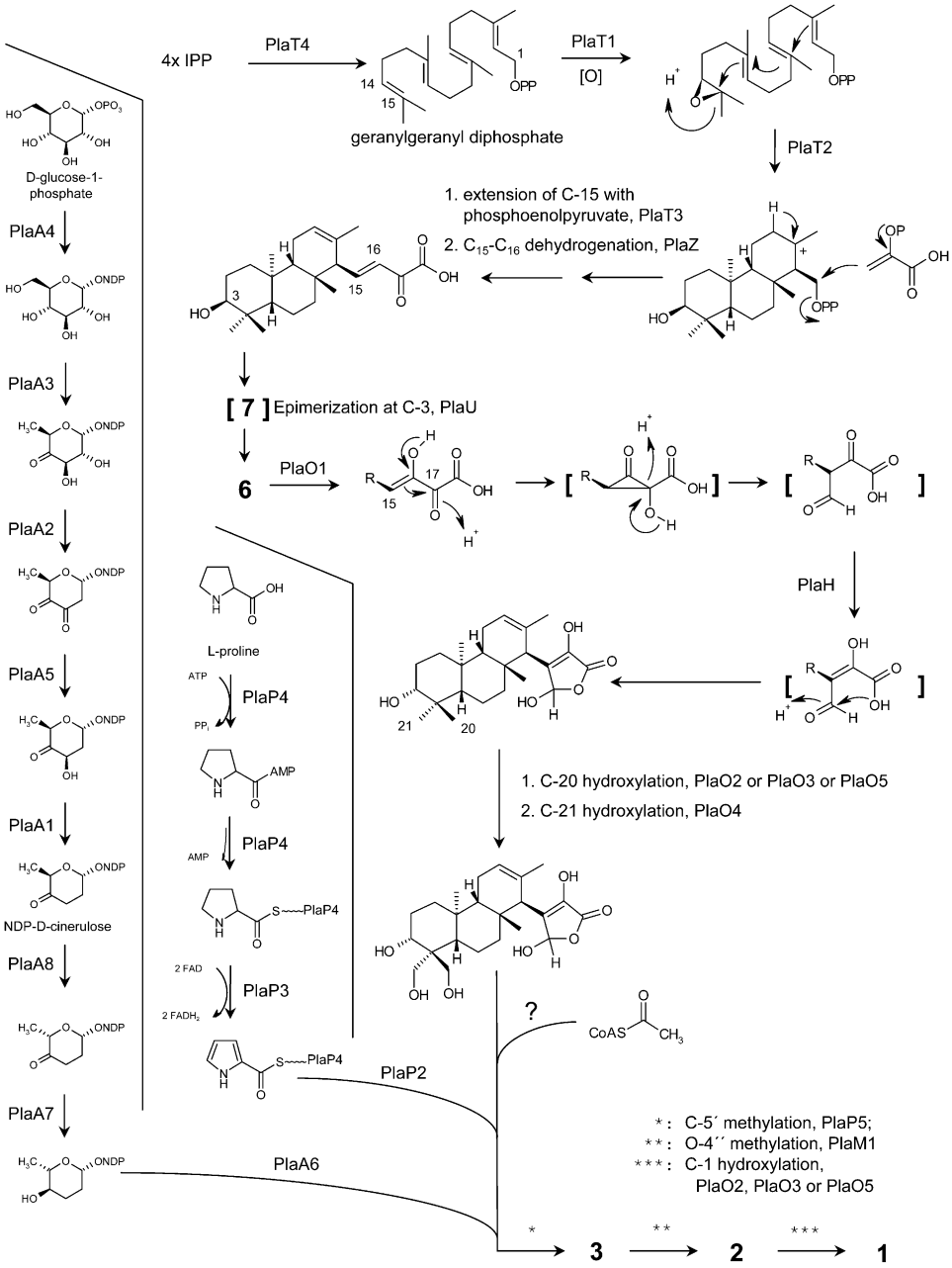

Figure 6. Proposed Biosynthetic Pathway for Phenalinolactone Formation

characteristic is the olefinic proton signal of H-12, which appears as an unresolved broad multiplett due to two allylic couplings to H-22 and H-14, respectively, and a ^{3}J-coupling to H-11.

The structure of the side chain observed in PL CD6 suggests that the biosynthetic precursor of the γ-butyrolactone is phosphoenolpyruvate, which gets attached to C-15 of the terpene backbone. The initial assumption, that **7** is the oxidized variant of **6**, was clearly confirmed by ^{1}H and ^{1}H/^{1}H-COSY analysis of **7**: the absence of the H-3 signal documents the oxidation of the secondary alcohol at C-3 toward the keto function (Figure 5). This is further reflected in the low field shift of the neighbored H-2$_{a/b}$ methylene signal from δ 1.60 in **6** toward δ 2.49 in **7**.

Model for Phenalinolactone Biosynthesis

The functional analysis of the *pla* gene cluster combined with the results from the structure elucidation of phenalinolactone intermediates allows a substantial proposal for the biosynthesis of **1**, as depicted in Figure 6. The pathway falls into the major parts of (1) terpene backbone formation and its extension with phosphoenolpyruvate, (2) modification and rearrangement of the phosphoenolpyruvate-derived side chain toward the γ-butyrolactone moiety, (3) biosynthesis of L-amicetose and pyrrole-2-carboxylic acid, and (4) group transfer reactions and late-step tailoring.

Based on sequence analysis, PlaT1–T6 comprise the enzymatic machinery to biosynthesize the

phenalinolactones scaffold, as represented in the structure of **6**. Feeding of D-[1-^{13}C]glucose to cultures of *Streptomyces* sp. Tü6071 clearly demonstrated that the isoprene building blocks for phenalinolactone biosynthesis derive from the nonmevalonate pathway. As all actinomycetes are equipped with the nonmevalonate pathway for isoprene production during primary metabolism [5], it is tempting to speculate why additional copies of the *dxp* and *hmbpp* synthase genes are located within the *pla* gene cluster. For the DXP synthase, a rate-limiting role in the nonmevalonate pathway could be suggested based on both assessment of its catalytic efficiency and the increased level of terpenoid production after overexpression [38]. Interestingly, the same immediate proximity of the *dxp* and the *hmbpp* synthase genes observed in the *pla* gene cluster is also present in the genomes of *Streptomyces coelicolor* and *Streptomyces avermitilis*, where the *hmbpp* synthase genes are located directly upstream of the *dxp* synthase genes as well. This conserved colocalization hints on a synergistic effect of both functions, potentially capable of enhancing isoprene production.

The GGDP synthase homolog PlaT4 would catalyze the consecutive head-to-tail condensations of four isoprene monomers toward GGDP, the phenalinolactones direct terpene precursor. The phenalinolactones hydroxyl function at C-3, which occurs at the equivalent position in eukaryotic sterols, and the presence of the squalene epoxidase homolog, PlaT1, suggest an epoxidation of the C-14/-15 double bond of GGDP prior to its cyclization. Indirect support for such a mechanism is 2-fold. First, the hydroxyl group at C-3 is already present in **6**, an intermediate whose structure seems to represent the stage in phenalinolactone formation immediately after the cyclization reaction. Second, the cyclase PlaT2 lacks the protonation motif DXDD, which would be essential for the direct protonation of the C-14/-15 double bond of GGDP without prior epoxidation [18].

The fact that the *plaO1* mutant produced, in addition to **6**, its 3-keto analog, **7**, raises the question whether an epimerization at C-3 takes place during this early stage of phenalinolactone biosynthesis. It may be speculated that the hydroxyl at C-3 emanates from the epoxide, primarily in the axial configuration. An epimerase would then oxidize C-3, yielding **7**, and then reduce the resulting ketone from the opposite face of the molecule, yielding **6**. This mode of direct epimerization was intensively studied for UDP-galactose-4-epimerases [39]. However, it can not be excluded that **7** is a shunt metabolite, emanating from accumulating **6** by the action of an unspecific dehydrogenase from outside the *pla* gene cluster.

The structure of the C_4 side chain observed in **6** suggests that pyruvate is the γ-butyrolactones precursor unit. The prenyltransferase homolog PlaT3 might be considered for the transfer of phosphoenolpyruvate to the terpene backbone, but it remains elusive whether this extension occurs before or after the cyclization reaction. As the next step, the dehydrogenation of the newly established C-C linkage would follow, giving the C-15/C-16 double bond. A candidate dehydrogenase for this reaction is encoded by *plaZ*. The subsequent hydroxylation of this double bond, resulting in the enol function at C-19, is likely to be catalyzed by the dioxygenase PlaO1, as indicated by the accumulation of the nonhydroxylated **6** in the *plaO1* mutant. Further steps toward the γ-butyrolactone portion remain very speculative. One potential route might be initiated by an intramolecular nucleophilic attack of C-15 on C-17, resulting in a cylopropanone intermediate. Ring opening would then yield the branched side chain with an aldehyde and an α-keto acid. Tautomerization of the α-keto group to the enol, potentially catalyzed by the isomerase PlaH, would be followed by the ring closure via hemi-acylal formation toward the γ-butyrolactone.

The molecular prerequisite for the decoration with the pyrrole and the sugar ligand is the oxidation of both methyl groups that are linked to the prochiral center at C-4. We could demonstrate that PlaO4 is responsible for the hydroxylation of the axial methyl group. Candidates for the hydroxylation of the equatorial methyl group are the remaining cytochrome P450 monoxygenases PlaO2, PlaO3, and PlaO5.

The final assembly of the phenalinolactones comprises the transfer of the pyrrole substituent to O-20, the *O*-glycosidic linkage of the L-amicetose to O-21, and the acetylation of O-3. The pyrrolyl and glycosyl transfer are presumably catalyzed by the putative acyltransferase PlaP2 and the putative glycosyltransferase PlaA6, respectively. However, for the acetyl transfer, no convincing candidate gene could be assigned; thus, it seems that the involved transferase is encoded from outside the *pla* gene cluster. The *C*-methylation at C-5 of the pyrrole moiety and the methylation of O-4 of the L-amicetose, catalyzed by PlaM1 and PlaP5, respectively, are regarded to be the last steps toward the biosynthesis of **2**. Finally, **2** gets converted to **1** through hydroxylation of C-1 by one of the cytochrome P450 monoxygenases (PlaO2, PlaO3, or PlaO5).

Significance

Phenalinolactones are novel tricyclic terpene metabolites from *Streptomyces* sp. Tü6071 with antibacterial activity. They exhibit a striking composition of structural elements of biosynthetic interest. With the characterization of the *pla* gene locus, we report here only the second biosynthetic gene cluster of a terpene natural product from *Streptomyces*, and the first one containing nonmevalonate pathway genes for isoprene biosynthesis. The functional analysis of the cluster, based on sequence comparison and gene inactivations, enabled us to propose a substantial model for the phenalinolactones biosynthetic pathway. We demonstrate that this pathway can be genetically manipulated to direct the generation of novel derivatives. This sets the basis for future studies on the engineering of more potent phenalinolactone analogs through combinatorial biosynthesis. The structure elucidation of an early-stage intermediate, which was isolated from a dioxygenase-deficient mutant strain, revealed that the γ-butyrolactone emanates from a C_4 side chain, which presumably derives from the attachment of phosphoenolpyruvate to the terpene backbone.

Experimental Procedures

Construction and Screening of a *Streptomyces* sp. Tü6071 Genomic Cosmid Library

DNA manipulations were performed according to standard procedures for *E. coli* [40] and *Streptomyces* [41]. A *Streptomyces* sp. Tü6071 genomic cosmid library was constructed in *E. coli* DH5α. For DNA extraction, mycelium was embedded in agarose, then the DNA was partially digested with Sau3AI and isolated, yielding fragments with an average size greater than 35 kbp. The fragments were ligated into cosmid pOJ436 digested with BamHI and in vitro-packaged with the Gigapack III Gold packaging extract kit according to the manufacturer' s handbook (Stratagene). Robotically produced high-density colony arrays (Hybond-N$^+$; Amersham Pharmacia) were utilized for the screening of 2304 cosmid clones with a strain-specific NDP-glucose-4,6-dehydratase gene probe following standard hybridization procedures. The gene probe was amplified with the oligonucleotide primers 5′-CSGGSGSSGCSGGSTT CATSGG-3′ (forward) and 5′-GGGWRCTGGYRSGGSCCGTAGTTG-3′ (reverse) by using genomic DNA from *Streptomyce* sp. Tü6071 as template (abbreviations according to standard IUPAC nomenclature for degenerate nucleotides).

Sequencing of the *pla* Gene Cluster

Cosmids 3-1O12 and 10-4D08 were sequenced by shotgun sequencing of a subclone library for each cosmid, consisting of 1.5–2.0 kbp fragments (obtained through shearing with a nebulizer) in pCR4blunt-TOPO (Invitrogen). DNA sequencing was carried out with an ABI Prism 3100 automated sequencer (Applied Biosystems). The raw sequence data were processed and assembled with the *phred/phrap/consed* software package (www.phrap.org). The annotation analysis of the sequence data was performed through database comparison with the BLAST search tools on the server of the National Center for Biotechnology Information, Bethesda, Maryland [42]. The sequence data reported here have been deposited in the GenBank database under the accession number DQ230532.

Culture Conditions

Streptomyces sp. Tü6071 was grown in NL111V liquid medium (2% lab lemco meat powder, 1% $CaCO_3$, 10% malt extract, pH adjusted to 7.2) dispensed in double-baffled flasks. The cultures were maintained at 28ºC and 180 rpm on a rotary incubator and harvested after 6–8 days. *E. coli* strains XL 1 blue and ET12567 were cultured in LB medium at 37ºC with the appropriate antibiotic selection at a final concentration of 100 μg ml^{-1} carbenicillin and 35 μg ml^{-1} apramycin.

Analysis of Phenalinolactone Production and Isolation of Derivatives

To assess phenalinolactone production of *Streptomyces* sp. Tü6071 wild-type and its mutants, 20 ml NL111V liquid media was inoculated from a sporulated plate culture and grown as described above. After 8 days, a 1 ml aliquot of the culture was extracted with 1 ml of ethyl acetate. The organic phase was evaporated to dryness with a Speed-Vac. The residue was redissolved in 200 μl DMSO 50% and clarified by centrifugation. HPLC/MS analysis was performed on an Agilent 1100 series system by ESI. The HPLC system was equipped with an Agilent ZORBAX SB C-18 column (5 μm particle size, 4.6 × 150 mm), maintained at 35ºC. Detection wavelength range of the diode array was set to 200–500 nm. The gradient profile consisted of solvent A (0.5% acetic acid in H_2O) and solvent B (0.5% acetic acid in CH_3CN). An initial hold for 3 min with 30% B was followed by a linear gradient with 35% B after 9 min, 60% B after 16 min, 85% B after 19 min, 95% B after 23 min, and held at 95% B for a further 7 min. The solvent flow rate was 0.7 ml min^{-1}.

For an upscaled phenalinolactone production, 1 liter NL111V liquid medium was equally dispensed into three 2 liter double-baffled Erlenmeyer flasks and inoculated with 3-day-old seed cultures. The cultures were agitated at 28ºC and 150 rpm. After 7 days, the fermentation was centrifuged to separate mycelia from the aqueous phase. The latter was extracted three times with equal volumes of ethyl acetate. The organic phase was dried, yielding from 200 to 400 mg crude extract. The crude extract was then adsorbed into a solid-phase extraction cartridge (SepPak C18; Waters Associates) and fractionated with a water/methanol gradient. Fractions containing phenalinolactone derivatives were pooled and applied for further isolation on an Agilent 1100 system with a semipreparative Zorbax Eclipse XDB-C18 column (5 μm particle size, 9.4 μm × 150 mm) utilizing mass guided-fraction collection. Phenalinolactone derivatives were yielded in the range of 1–2 mg per 1 liter fermentation broth.

Structure Elucidation

High-resolution ESI (HRESI) mass spectra were acquired with a Micromass QTOF2 mass spectrometer. NMR spectra were recorded at a ^{1}H resonance frequency of 500 MHz (Bruker DRX 500) and 400 MHz (Bruker DRX 400). Standard parameters were used for 1D and 2D NMR spectra, which included ^{1}H, ^{13}C, ^{1}H/^{1}H-correlated spectroscopy (COSY), heteronuclear single-quantum coherence (HSQC), and heteronuclear multiple-bond correlation (HMBC). All chemical shifts were referenced to residual $CHCl_3$ (**2**, **3**) and MeOH (**4**, **6**, **7**), respectively.

Phenalinolactone D (2)

^{1}H NMR ($CDCl_3$) δ (multiplicity, assignment): 0.98 (s, H24); 1.08 (s, H1a); 1.10 (m, H7a); 1.12 (m, H9); 1.17 (s, H22); 1.24 (d, H6″); 1.30 (brd, H5); 1.58–1.72 (m, H2a); 1.58–1.72 (m, H2b); 1.62 (brs, H23); 1.67 (m, H7b); 1.72 (m, H2″a); 1.72–1.85 (m, H3″a); 1.72–1.85 (m, H3″b); 1.77 (m, H6a); 1.87 (m, H1b); 1.87 (m, H6b); 1.89 (m, H2″b); 2.04 (s, H26); 2.09 (m, H11b); 2.30 (m, H11a); 2.33 (brs, H6′); 3.01 (ddd, H4″); 3.41 (brs, H14); 3.41 (d, H21b); 3.51 (s, H7″); 3.84 (d, H20b); 3.89 (dq, H5″); 4.42 (d, H21a); 4.83 (d, H20a); 4.62 (d, H1″); 5.04 (dd, H3); 5.53 (brs, H12); 5.86 (d, H16); 5.97 (dd, H4′); 6.85 (dd, H3′); 7.15 (d, 16-OH); 9.03 (brs, NH); ^{13}C NMR ($CDCl_3$) δ: 13.2 (C6′); 14.3 (C24); 17.7 (C6″); 20.7 (C6); 21.3 (C26); 22.1 (C23); 23.1 (C11); 23,4 (C2); 23.8 (C3″); 27.6 (C22); 29.3 (C2″); 38,2 (C1); 38.4 (C10); 39.2 (C8); 40.2 (C14); 40.5 (C7); 45.1 (C4); 49.1 (C5); 54.7 (C9); 56.7 (C7″); 62.6 (C20); 68.6 (C5″); 68.8 (C21); 73.9 (C3); 81.6 (C4″); 98.1 (C1″); 98.5 (C16); 109.1(C4′); 116.6 (C3′); 120.9 (C2′); 122.2 (C12); 129.8 (C15); 132.4 (C13); 134.1 (C5′); 138.8 (C19); 160.3 (C1′); 169.1 (C18); 170.5 (C25).

Phenalinolactone CD1 (3)

^{1}H NMR ($CDCl_3$) δ (multiplicity, assignment): 0.98 (s, H24); 1.09 (s, H1a); 1.10 (m, H7a); 1.10 (m, H9); 1.18 (s, H22); 1.26 (d, H6″); 1.30 (brd, H5); 1.58–1.72 (m, H2a); 1.58–1.72 (m, H2b); 1.62 (brs, H23); 1.72–1.85 (m, H3″a); 1.72–1.85 (m, H3″b); 1.75 (m, H2″a); 1.78 (m, H7b); 1.80 (m, H6a); 1.87 (m, H1b); 1.90 (m, H2″b); 1.90 (m, H6b); 2.04 (s, H26); 2.05 (m, H11b); 2.28 (m, H11a); 2.33 (brs, H6′); 3.40 (brs, H14); 3.41 (d, H21b); 3.48 (ddd, H4″); 3.85 (d, H20b); 3.86 (dq, H5″); 4.42 (d, H21a); 4.84 (d, H20a); 4.62 (d, H1″); 5.03 (dd, H3); 5.54 (brs, H12); 5.93 (s, H16); 5.97 (dd, H4′); 6.85 (dd, H3′); 9.03 (brs, NH); ^{13}C NMR ($CDCl_3$) δ: 13.2 (C6′); 14.3 (C24); 17.6 (C6″); 20.7 (C6); 21.3 (C26); 22.1 (C23); 23.1 (C11); 23.4 (C2); 27.6 (C22); 28.1 (C3″); 29.7 (C2″); 38.3 (C1); 38.4 (C10); 39.2 (C8); 40.3 (C14); 40.5 (C7); 45.1 (C4); 49.1 (C5); 54.7 (C9); 62.7 (C20); 68.9 (C21); 69.5 (C5″);72.8 (C4″); 73.9 (C3); 98.2 (C1″); 98.6 (C16); 109.1(C4′); 116.7 (C3′); 120.9 (C2′); 122.3 (C12); 130.0 (C15); 132.3 (C13); 134.1 (C5′); 139.0 (C19); 160.4 (C1′); 169.1 (C18); 170.5 (C25).

Phenalinolactone CD2 (4)

^{1}H NMR (CD_3OD) δ (multiplicity, assignment, coupling constants, HMBCs [* indicates indirectly observed via HSQC/HMBC; ** indicates overlap with solvent]): 0.79 (s, H21, C3, C4, C5, C20); 0.96 (s, H22, C7, C9, C14); 1.00 (m, H1a); 1.00 (m, H7b); 1.04 (s, H24, C1, C5, C9, C10); 1.11 (m, H9, C12, C24); 1.40 (m, H5); 1.50 (m, H6a); 1.50 (m, H6b); 1.60–1.85 (m, H2a); 1.60–1.85 (m, H2b); 1.61(brs, H23, C12, C13); 1.75 (m, H7a); 1.85 (m, H1b); 2.15 (m, H11b); 2.27 (brs, H6' , C4′, C5′); 2.30 (m, H11a); 3.35 (m, H14); 3.67 (dd, H3, *J* = 5 Hz, 12 Hz); 4.04 (d, H20a, *J* = 11.5 Hz); 4.11 (d, H20b, *J* = 11.5 Hz, C-1′, C3, C5); 5.47 (brs, H12); 5.91 (d, H4' , *J* = 3.5 Hz, C-2′, C-3′, C-5′); 5,93 (s, H16); 6.75 (d, H3′, *J* = 3.5 Hz, C-2′, C-4′, C-5′); ^{13}C NMR (CD_3OD) δ: 12.9 (C21); 12.9 (C6'); 15.3 (C24); 18.9 (C6); 22.7 (C23); 23.8 (C11); 27.6 (C2); 29 (C22*); 39.5 (C1); 40 (C14*); 40.1 (C10); 40.2 (C7); 40.2 (C8); 43 (C4*); 50 (C5**); 56 (C9*); 66.1 (C20); 72.7 (C3); 101 (C16*); 109.6 (C4'); 117.5 (C3′); 122.0 (C12); 123.4 (C2′); 136.1 (C5′); 162.5 (C1'). Carbon signals at C13, C15, C18, and C19 were not detectable due to low quantity.

Phenalinolactone CD6 (6)

^{1}H NMR (CD_3OD) δ (multiplicity, assignment, coupling constants, HMBCs [* indicates assignments exchangeable; ** indicates overlap with solvent; *** indicates long-range couplings and ^{13}C-signals

detectable only at 248K]): 0.78 (s, H20, C3, C4, C5, C19), 0.86 (m, H5, C20), 0.91 (s, H21, C7, C8, C9, C14), 0.94 (s, H23, C1, C5, C9), 0.95 (m, H7a), 0.96 (s, H19, C3, C4, C5, C20), 1.06 (brd, H9, C8, C11, C12, C21, C23), 1.08 (m, H1a), 1.54 (brs, H22, C12, C13, C14), 1.60 (m,, H2ab), 1.60 (m, H6ab), 1.80 (m, H1b), 1.80 (m, H7b), 2.10 (brd, H11a, J = 15 Hz,), 2.20 (brd, H11b, J = 15 Hz), 3.13 (dd, H3, J = 5, 12 Hz, C20), 3.15 (brd, H14, J = 11 Hz, C16***), 5.51 (brs, H12), 6.29 (d, H16, J = 16 Hz, C17***, C18***), 6.82 (dd, H15, J = 11, 16 Hz, C17***); ^{13}C NMR (CD_3OD) δ:15.2 (C23), 16.4 (C20), 19.0 (C6), 23.3 (C22), 23.6 (C11), 27.9 (C21), 28.1 (C2), 28.8 (C19), 37.8 (C8), 39.4 (C1), 40.0 (C4*), 40.0 (C10*), 40.3 (C7*), 50 (C14**), 56.1 (C9), 57.1 (C5), 79.7 (C3), 123.8 (C12), 132.0 (C16), 133.3 (C13), 156.0 (C15), 168.5 (C18***), 191.0 (C17***).

Phenalinolactone CD7 (7)

^{1}H NMR (CD_3OD) δ (multiplicity, assignment, coupling constants [* indicates indirectly observed through ^{1}H, ^{1}H-COSY; ** indicates assignments exchangeable]): 0.80–1.80 (m, H5, H6ab, H7ab), 0.95 (s, H21**), 0.97 (s, H23**), 1.07 (s, H20**), 1.08 (s, H19**), 1.08 (m, H1a), 1.15 (brd, H9*), 1.57 (brs, H22), 1.60 (m, H6ab), 1.80 (m, H1b), 1.80 (m, H7b), 2.10 (brd, H11a, J = 15 Hz,), 2.20 (brd, H11b), 2.49 (dd, H2ab), 3.18 (brd, H14*, J = 11 Hz), 5.53 (brs, H12), 6.32 (d, H16, J = 16 Hz), 6.82 (dd, H15, J = 11, 16 Hz).

Feeding of D-[1-^{13}C]glucose and Quantification of Enrichment

Double-baffled Erlenmeyer flasks (3 × 2 liter), each containing 330 ml NL 19 medium (2% soy flour, 2% mannitol, pH adjusted to 7.2), were inoculated with a 32-hr-old *Streptomyces* sp. Tü6071 seed culture. The cultures were grown in a rotary incubator at 28ºC and 180 rpm. D-[1-^{13}C]glucose was fed in equal portions after 96, 120, 144, and 168 hr in a total amount of 2 g/1000 ml of culture. The fermentation was harvested 8 days after inoculation. The extraction and isolation of labeled phenalinolactone D was done as described above. To quantify the relative ^{13}C-enrichments resulting from exogenously supplied D-[1-^{13}C]glucose, an average normalization factor was calculated from carbon resonances expected to be unlabeled. This was done by dividing the average intensity of the selected signal from the natural abundance spectrum by the average intensity of the same signal from the ^{13}C-enriched spectrum. All resonances in the ^{13}C-enriched spectrum were then multiplied by this normalization value, giving the relative enrichment.

Generation of Mutant Strains of *Streptomyces* sp. Tü6071

DNA manipulation was carried out with *E. coli* XL-1 Blue MRF′ (Stratagene) as host strain. To generate the mutants *Streptomyces* sp. Tü6071 ΔplaM1, ΔplaO1, ΔplaO4, ΔplaT1, ΔplaT2, and ΔplaT3 by means of insert-directed homologous recombination, the target genes were amplified by PCR, including flanking DNA of about 1.0 kbp up- and downstream of the start and stop codon, respectively. Cosmids 3-1O12 and 10-4D08 were used as template. The primer sequences and a detailed protocol for the generation of the final plasmids are available in the Supplemental Data. The final pKC1132-derived plasmids were introduced into *Streptomyces* sp. Tü6071 by intergeneric conjugation with the methylation-deficient donor strain *E. coli* ET12567 (*dam*$^-$, *dcm*$^-$, *hsd*S, Cm^R) [43] containing the conjugative vector pUZ8002 (see below). Exconjugants were selected for the integration of the vector with apramycin. Resistant colonies (single crossover) were grown nonselectively on HA agar plates for several generations. Spores of single colonies were dissected by replica plating for individuals that had lost the vector (double crossover). Single and double crossover recombination events were screened by PCR (see Supplemental Data).

Intergeneric Conjugation

A colony of the donor strain *E. coli* ET12567 (pUZ8002) containing pKC1132-derived inactivation plasmids or pSET152 constructs for complementation was plated out on LB agar containing chloramphenicol (25 μg ml^{-1}), kanamycin (30 μg ml^{-1}), and apramycin (35 μg ml^{-1}), and incubated at 37ºC overnight. Donor cells were scratched from the abundantly covered plate and suspended in a spore suspension of the recipient strain *Streptomyces* sp. Tü6071 prepared with HA liquid media. The mixture was spread on MS agar, incubated for 12–14 hr at 28ºC, and overlaid with 1 ml water containing 0.8 mg nalidixic acid and 1.2 mg apramycin. The plates were further incubated at 28ºC. Exconjugants were transferred on TSB agar containing nalidixic acid (35 μg ml^{-1}) and apramycin (35 μg ml^{-1}).

Complementation of *Streptomyces* sp. Tü6071 Mutant Strains

Mutant strains were complemented with pSET152-derived constructs (see Supplemental Data) carrying only the target gene behind the strong *ermE* promotor. The complementation plasmids were introduced in the respective mutant strains by conjugation, and exconjugants were selected with apramycin. Resistant colonies were grown nonselectively and the restored wild-type production was assessed by HPLC/MS analyses.

Supplemental Data

Supplemental Data, including information regarding vectors, PCR conditions, and generation and complementation of mutant strains of *Streptomyces* sp. Tü6071, are available online at http://www.chembiol.com/cgi/content/full/13/4/365/DC1/.

Acknowledgments

We thank Prof. Dr. Michael Müller, Albert-Ludwigs-Universität Freiburg, for helpful discussions and for providing the NMR facilities. Dr. Tilmann Weber, Eberhard-Karls-Universität Tübingen, is gratefully acknowledged for his support in processing the sequence raw data. We further thank Volker Brecht, Albert-Ludwigs-Universität Freiburg, for recording the NMR spectra, and Dr. Sven-Eric Wohlert, Combinature Biopharm AG Berlin, for high-resolution MS. This work was supported by the BMBF (GenoMik) grant to A.B.

Received: October 11, 2005
Revised: January 12, 2006
Accepted: January 27, 2006
Published: April 21, 2006

References

1. Challis, G.L., and Hopwood, D.A. (2003). Synergy and contingency as driving forces for the evolution of multiple secondary metabolite production by *Streptomyces* species. Proc. Natl. Acad. Sci. USA *100*, 14555–14561.
2. Wendt, K.U., and Schulz, G.E. (1998). Isoprenoid biosynthesis: manifold chemistry catalyzed by similar enzymes. Structure *6*, 127–133.
3. Hoeksema, H., and Smith, C.G. (1961). Novobiocin. Prog. Ind. Microbiol. *3*, 91–139.
4. Takeuchi, S., Ogawa, Y., and Yonehara, H. (1969). The structure of pentalenolactone (PA-132). Tetrahedron Lett. *32*, 2737–2740.
5. Kuzuyama, T., and Seto, H. (2003). Diversity of the biosynthesis of the isoprene units. Nat. Prod. Rep. *20*, 171–183.
6. Hamano, Y., Dairi, T., Yamamoto, M., Kawasaki, T., Kaneda, K., Kuzuyama, T., Itoh, N., and Seto, H. (2001). Cloning of a gene cluster encoding enzymes responsible for the mevalonate pathway from a terpenoid-antibiotic-producing *Streptomyces* strain. Biosci. Biotechnol. Biochem. *65*, 1627–1635.
7. Dairi, T., Hamano, Y., Kuzuyama, T., Itoh, N., Furihata, K., and Seto, H. (2001). Eubacterial diterpene cyclase genes essential for production of the isoprenoid antibiotic terpentecin. J. Bacteriol. *183*, 6085–6094.
8. Gebhardt, K. (2002). Naturstoffe aus endosymbiontischen Mikroorganismen von Arthropoden und aus Mikroorganismen terrestrischer Habitate. PhD thesis, Institute of Microbiology. University of Tübingen, Tübingen, Germany.
9. Meyer, S.W. (2003). Strukturaufklärung der Phenalinolactone und Beiträge zur Biosynthese der Hexacyclinsäure. PhD thesis, Institute of Organic and Biomolecular Chemistry, University of Göttingen, Göttingen, Germany (http://webdoc.sub.gwdg.de/diss/2004/meyer).
10. Randazzo, A., Debitus, C., Minale, L., Garcia, P.P., Alcaraz, M.J., Paya, M., and Gomez-Paloma, L. (1998). Petrosaspongiolides M-R: new potent and selective phospholipase A2 inhibitors from the New Caledonian marine sponge *Petrosaspongia nigra*. J. Nat. Prod. *61*, 571–575.
11. Monti, M.C., Casapullo, A., Riccio, R., and Gomez-Paloma, L. (2004). Further insights on the structural aspects of PLA(2)

inhibition by gamma-hydroxybutenolide-containing natural products: a comparative study on petrosaspongiolides M-R. Bioorg. Med. Chem. *12*, 1467–1474.

12. Tsai, F.T., Singh, O.M., Skarzynski, T., Wonacott, A.J., Weston, S., Tucker, A., Pauptit, R.A., Breeze, A.L., Poyser, J.P., O' Brien, R., et al. (1997). The high-resolution crystal structure of a 24-kDa gyrase B fragment from *E. coli* complexed with one of the most potent coumarin inhibitors, clorobiocin. Proteins *28*, 41–52.
13. Bode, H.B., Zeggel, B., Silakowski, B., Wenzel, S.C., Reichenbach, H., and Müller, R. (2003). Steroid biosynthesis in prokaryotes: identification of myxobacterial steroids and cloning of the first bacterial 2,3(S)-oxidosqualene cyclase from the myxobacterium *Stigmatella aurantiaca*. Mol. Microbiol. *47*, 471–481.
14. Trefzer, A., Salas, J.A., and Bechthold, A. (1999). Genes and enzymes involved in deoxysugar biosynthesis in bacteria. Nat. Prod. Rep. *16*, 283–299.
15. Bibb, M.J., Findlay, P.R., and Johnson, M.W. (1984). The relationship between base composition and codon usage in bacterial genes and its use for the simple and reliable identification of protein-coding sequences. Gene *30*, 157–166.
16. Kollas, A.K., Duin, E.C., Eberl, M., Altincicek, B., Hintz, M., Reichenberg, A., Henschker, D., Henne, A., Steinbrecher, I., Ostrovsky, D.N., et al. (2002). Functional characterization of GcpE, an essential enzyme of the non-mevalonate pathway of isoprenoid biosynthesis. FEBS Lett. *532*, 432–436.
17. Pearson, A., Budin, M., and Brocks, J.J. (2003). Phylogenetic and biochemical evidence for sterol synthesis in the bacterium *Gemmata obscuriglobus*. Proc. Natl. Acad. Sci. USA *100*, 15352–15357.
18. Wendt, K.U., Poralla, K., and Schulz, G.E. (1997). Structure and function of a squalene cyclase. Science *277*, 1811–1815.
19. Perez, M., Lombo, F., Zhu, L., Gibson, M., Brana, A.F., Rohr, J., Salas, J.A., and Mendez, C. (2005). Combining sugar biosynthesis genes for the generation of L- and D-amicetose and formation of two novel antitumor tetracenomycins. Chem. Commun. *12*, 1604–1606.
20. Hoffmeister, D., Ichinose, K., Domann, S., Faust, B., Trefzer, A., Dräger, G., Kirschning, A., Fischer, C., Künzel, E., Bearden, D., et al. (2000). The NDP-sugar co-substrate concentration and the enzyme expression level influence the substrate specificity of glycosyltransferases: cloning and characterization of deoxysugar biosynthetic genes of the urdamycin biosynthetic gene cluster. Chem. Biol. *7*, 821–831.
21. Sun, Y., Zhou, X., Dong, H., Tu, G., Wang, M., Wang, B., and Deng, Z. (2003). A complete gene cluster from *Streptomyces nanchangensis* NS3226 encoding biosynthesis of the polyether ionophore nanchangmycin. Chem. Biol. *10*, 431–441.
22. Garneau, S., Dorrestein, P.C., Kelleher, N.L., and Walsh, C.T. (2005). Characterization of the formation of the pyrrole moiety during clorobiocin and coumermycin A1 biosynthesis. Biochemistry *44*, 2770–2780.
23. Westrich, L., Heide, L., and Li, S.M. (2003). CloN6, a novel methyltransferase catalysing the methylation of the pyrrole-2-carboxyl moiety of clorobiocin. ChemBioChem *4*, 768–773.
24. Xu, H., Kahlich, R., Kammerer, B., Heide, L., and Li, S.M. (2003). CloN2, a novel acyltransferase involved in the attachment of the pyrrole-2-carboxyl moiety to the deoxysugar of clorobiocin. Microbiol. *149*, 2183–2191.
25. Mendes, M.V., Anton, N., Martin, J.F., and Aparicio, J.F. (2005). Characterization of the polyene macrolide P450 epoxidase from *Streptomyces natalensis* that converts de-epoxypimaricin into pimaricin. Biochem. J. *386*, 57–62.
26. Hausinger, R.P. (2004). FeII/alpha-ketoglutarate-dependent hydroxylases and related enzymes. Crit. Rev. Biochem. Mol. Biol. *39*, 21–68.
27. Zhang, Z., Ren, J., Stammers, D.K., Baldwin, J.E., Harlos, K., and Schofield, C.J. (2000). Structural origins of the selectivity of the trifunctional oxygenase clavaminic acid synthase. Nat. Struct. Biol. *7*, 127–133.
28. Wietzorrek, A., and Bibb, M. (1997). A novel family of proteins that regulates antibiotic production in streptomycetes appears to contain an OmpR-like DNA-binding fold. Mol. Microbiol. *25*, 1181–1184.
29. Oliynyk, M., Stark, C.B., Bhatt, A., Jones, M.A., Hughes-Thomas, Z.A., Wilkinson, C., Oliynyk, Z., Demydchuk, Y., Staunton, J., and Leadlay, P.F. (2003). Analysis of the biosynthetic gene cluster for the polyether antibiotic monensin in *Streptomyces cinnamonensis* and evidence for the role of *mon*B and *monC* genes in oxidative cyclization. Mol. Microbiol. *49*, 1179–1190.
30. Mosbacher, T.G., Bechthold, A., and Schulz, G.E. (2003). Crystal structure of the avilamycin resistance-conferring methyltransferase AviRa from *Streptomyces viridochromogenes*. J. Mol. Biol. *329*, 147–157.
31. Wagner, U.G., Petersen, E.I., Schwab, H., and Kratky, C. (2002). EstB from *Burkholderia gladioli*: a novel esterase with a β-lactamase fold reveals steric factors to discriminate between esterolytic and β-lactam cleaving activity. Protein Sci. *11*, 467–478.
32. Olano, C., Wilkinson, B., Sanchez, C., Moss, S.J., Sheridan, R., Math, V., Weston, A.J., Brana, A.F., Martin, C.J., Oliynyk, M., et al. (2004). Biosynthesis of the angiogenesis inhibitor borrelidin by *Streptomyces parvulus* Tu4055: cluster analysis and assignment of functions. Chem. Biol. *11*, 87–97.
33. Brzostowicz, P.C., Blasko, M.S., and Rouviere, P.E. (2002). Identification of two gene clusters involved in cyclohexanone oxidation in *Brevibacterium epidermidis* strain HCU. Appl. Microbiol. Biotechnol. *58*, 781–789.
34. Knoss, W., Reuter, B., and Zapp, J. (1997). Biosynthesis of the labdane diterpene marrubiin in *Marrubium vulgare* via a non-mevalonate pathway. Biochem. J. *326*, 449–454.
35. Weitnauer, G., Hauser, G., Hofmann, C., Linder, U., Boll, R., Pelz, K., Glaser, S.J., and Bechthold, A. (2004). Novel avilamycin derivatives with improved polarity generated by targeted gene disruption. Chem. Biol. *11*, 1403–1411.
36. Li, S.M., Westrich, L., Schmidt, J., Kuhnt, C., and Heide, L. (2002). Methyltransferase genes in *Streptomyces rishiriensis*: new coumermycin derivatives from gene-inactivation experiments. Microbiol. *148*, 3317–3326.
37. Shigemori, H., Komaki, H., Yazawa, K., Mikami, Y., Nemoto, A., Tanaka, Y., Sasaki, T., In, Y., Ishida, T., and Kobayashi, J. (1998). Brasilicardin A: a novel tricyclic metabolite with potent immunosuppressive activity from actinomycete *Nocardia brasiliensis*. J. Org. Chem. *63*, 6900–6904.
38. Kuzuyama, T., Takagi, M., Takahashi, S., and Seto, H. (2000). Cloning and characterization of 1-deoxy-D-xylulose 5-phosphate synthase from *Streptomyces* sp. Strain CL190, which uses both the mevalonate and nonmevalonate pathways for isopentenyl diphosphate biosynthesis. J. Bacteriol. *182*, 891–897.
39. Field, R.A., and Naismith, J.H. (2003). Structural and mechanistic basis of bacterial sugar nucleotide-modifying enzymes. Biochemistry *42*, 7637–7647.
40. Sambrook, J., Fritsch, E.F., and Maniatis, T. (1989). Molecular Cloning: A Laboratory Manual (Cold Spring Harbor, NY: Cold Spring Harbor Laboratory Press).
41. Hopwood, D.A., Bibb, M.J., Chater, K.F., Kieser, T., Bruton, C.J., Kieser, H.M., Lydiate, D.J., Smith, C.P., Ward, J.M., and Schrempf, H. (1985). Genetic Manipulation of *Streptomyces*: A Laboratory Manual (Norwich, UK: The John Innes Foundation).
42. Altschul, S.F., Madden, T.L., Schaffer, A.A., Zhang, J., Zhang, Z., Miller, W., and Lipman, D.J. (1997). Gapped BLAST and PSI-BLAST: a new generation of protein database search programs. Nucleic Acids Res. *25*, 3389–3402.
43. MacNeil, D.J., Gewain, K.M., Ruby, C.L., Dezeny, G., Gibbons, P.H., and MacNeil, T. (1992). Analysis of *Streptomyces avermitilis* genes required for avermectin biosynthesis utilizing a novel integration vector. Gene *111*, 61–68.
44. Westrich, L., Domann, S., Faust, B., Bedford, D., Hopwood, D.A., and Bechthold, A. (1999). Cloning and characterization of a gene cluster from *Streptomyces cyanogenus* S136 probably involved in landomycin biosynthesis. FEMS Microbiol. Lett. *170*, 381–387.
45. Lombo, F., Siems, K., Brana, A.F., Mendez, C., Bindseil, K., and Salas, J.A. (1997). Cloning and insertional inactivation of *Streptomyces argillaceus* genes involved in the earliest steps of biosynthesis of the sugar moieties of the antitumor polyketide mithramycin. J. Bacteriol. *179*, 3354–3357.
46. Pojer, F., Li, S.M., and Heide, L. (2002). Molecular cloning and sequence analysis of the clorobiocin biosynthetic gene cluster:

new insights into the biosynthesis of aminocoumarin antibiotics. Microbiol. *148*, 3901–3911.
47. Endoh, T., Kasuga, K., Horinouchi, M., Yoshida, T., Habe, H., Nojiri, H., and Omori, T. (2003). Characterization and identification of genes essential for dimethyl sulfide utilization in *Pseudomonas putida* strain DS1. Appl. Microbiol. Biotechnol. *62*, 83–91.
48. Sakakibara, J., Watanabe, R., Kanai, Y., and Ono, T. (1995). Molecular cloning and expression of rat squalene epoxidase. J. Biol. Chem. *270*, 17–20.
49. Piel, J., Hertweck, C., Shipley, P.R., Hunt, D.M., Newman, M.S., and Moore, B.S. (2000). Cloning, sequencing and analysis of the enterocin biosynthesis gene cluster from the marine isolate '*Streptomyces maritimus*': evidence for the derailment of an aromatic polyketide synthase. Chem. Biol. *7*, 943–955.
50. Brikun, I.A., Reeves, A.R., Cernota, W.H., Luu, M.B., and Weber, J.M. (2004). The erythromycin biosynthetic gene cluster of *Aeromicrobium erythreum*. J. Ind. Microbiol. Biotechnol. *31*, 335–344.
51. Draeger, G., Park, S.H., and Floss, H.G. (1999). Mechanism of the 2-deoxygenation step in the biosynthesis of the deoxyhexose moieties of the antibiotics granaticin and oleandomycin. J. Am. Chem. Soc. *121*, 2611–2612.
52. Blanco, G., Fernandez, E., Fernandez, M.J., Brana, A.F., Weissbach, U., Künzel, E., Rohr, J., Mendez, C., and Salas, J.A. (2000). Characterization of two glycosyltransferases involved in early glycosylation steps during biosynthesis of the antitumor polyketide mithramycin by *Streptomyces argillaceus*. Mol. Gen. Genet. *262*, 991–1000.
53. Bate, N., Butler, A.R., Smith, I.P., and Cundliffe, E. (2000). The mycarose-biosynthetic genes of *Streptomyces fradiae*, producer of tylosin. Microbiol. *146*, 139–146.
54. Betlach, M.C., Kealey, J.T., Ashley, G.W., and McDaniel, R. (1998). Characterization of the macrolide P-450 hydroxylase from *Streptomyces venezuelae* which converts narbomycin to picromycin. Biochemistry *37*, 14937–14942.
55. Chen, S., von Bamberg, D., Hale, V., Breuer, M., Hardt, B., Müller, R., Floss, H.G., Reynolds, K.A., and Leistner, E. (1999). Biosynthesis of ansatrienin (mycotrienin) and naphthomycin: identification and analysis of two separate biosynthetic gene clusters in *Streptomyces collinus* Tu 1892. Eur. J. Biochem. *261*, 98–107.

Accession Numbers

The sequence data reported here has been deposited in the GenBank database under the accession code DQ230532.